

## Solvent effect on the excited state of stilbene dendrimers bearing phenylacetylene groups

Yoshinobu Nishimura\* and Tatsuo Arai\*

Faculty of Pure and Applied Sciences, University of Tsukuba, Tsukuba, Ibaraki 305-8571, Japan

**ABSTRACT:** We studied the characteristics of emissive state of the first (*p*-G1) and second (*p*-G2) generation of phenylacetylene dendrimers bearing stilbene as a core by using time-resolved fluorescence spectroscopy in cyclohexane (c-Hex) and *N,N*-dimethylformide (DMF), which are nonpolar and polar solvents, respectively. Time-dependent red-shift of emission spectra *p*-G2 both in c-Hex and DMF was observed in comparison with *p*-G1. Besides, the time constant of red-shift of spectra was found to be larger in DMF than in c-Hex. This indicates that the emissive state of *p*-G2 has a polar character in DMF as a result of charge delocalization from core to peripheral dendrons followed by stabilization of emissive state.

Dendrimers, which are supramolecular compounds possessing a well-defined conformation, have been attracting many kinds of favorable attention such as light harvesting, nonlinear effect, transistor and medical usages by introducing functional groups to peripheries<sup>1-3</sup>. Useful dendrimer frameworks assembled by various functional building blocks may allow us to achieve these functionalities. For example, control of electronic interaction between chromophores was reported for nitrogen-cored distyrylbenzene dendrimers by its generation as a candidate for light-emitting diode<sup>4</sup>. In addition, intramolecular energy migration is one of the much interesting research field because of relevance to light-harvesting antenna such as rylene dyes<sup>5</sup>. The interaction between core and peripheral part in a dendritic molecule has been investigated by many researchers<sup>6, 7</sup>. The energy transfer mechanism in these moieties has been ascribed to Förster and Dexter mechanisms, which correspond to resonance and exchange interactions, respectively<sup>8</sup>. Since the efficiency of energy transfer depends on distance and orientation of energy donor and acceptor, it is essential for covalent linkage between energy donor and acceptor fixed by particular geometry to achieve optimal orientation between transition moments, where the main interaction is reported to be through space and through bond involving intervening  $\sigma$  bonds<sup>9, 10</sup>. Theoretical works concerning phenylacetylene dendrimers have been done to interpret the kinetics of intramolecular energy transfer by combination of Förster mechanism and exciton model<sup>11-13</sup>. The aim of present study is focused on elucidation of relaxation process in the excited state of the dendrimer linked by phenylacetylene units. In this sense, solvent polarity may affect the decay kinetics following fluorescence spectral shift caused by prolonged excitation delocalization; i.e., transient dipole moment. Time-resolved studies have also been performed to understand the kinetics of energy migration and nonlinear effect in the singlet excited state by using ultrafast anisotropy and three-pulse photon echo measurements<sup>14</sup>. Thus, time-resolved fluorescence spectroscopy is an important tool to analyze the energy transfer mechanism, since

kinetic parameters and spectral profiles can be derived by the analysis. For example, the dynamic Stokes shift of time-resolved emission spectra gives us the information of the excited state such as structural relaxation.

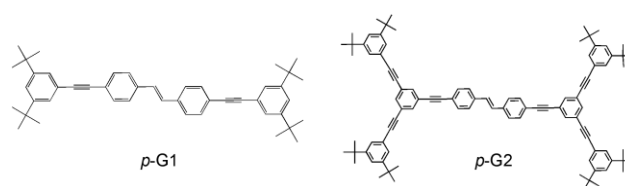


**Figure 1.** Structures of *p*-G1 and *p*-G2 examined in the present study.

As reported previously, small solvent effect was observed in relation to the time constant and time-resolved spectra with excitation at 410 nm, which excited at the red-edge of the absorption spectra<sup>15</sup>. In this study, 375-nm excitation allowed us to measure more precise experiment about time-resolved spectra so as to observe whole range of emission spectra. As a result, we successfully observed the dynamics Stokes shift of time-resolved spectra within 1 ns after excitation, which clearly depended on the solvent polarity; nonpolar and polar solvents for c-Hex and DMF, respectively. This indicates that *p*-G<sub>n</sub> may have a polar structure in the excited state as an emissive state.

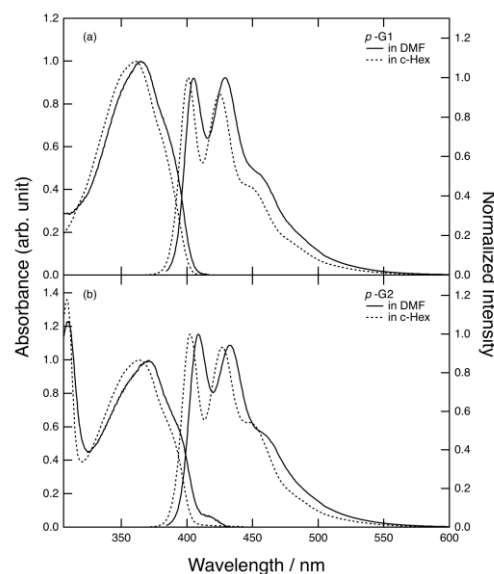


**Figure 2.** Absorption and emission spectra of (a) *p*-G1 and (b) *p*-G2 in DMF (solid line) and cyclohexane (dashed line). Excitation wavelength was 375 nm.

\*To whom correspondence should be addressed.  
E-mail: nishimura@chem.tsukuba.ac.jp

*p*-G1 and *p*-G2 shown in Fig. 1 were synthesized according to the literature<sup>16</sup>. Details were described in a previous paper.<sup>15</sup> Sample solutions were prepared in cyclohexane (c-Hex, Kanto Chemical) and *N,N*-dimethylformide (DMF, Kanto Chemical) and deoxygenated by bubbling highly purified argon (>99.999%). Absorption spectra were recorded with Shimadzu UV-1600 spectrophotometer. Fluorescence and excitation spectra were measured with Hitachi F-4500 fluorimeter.

Fluorescence decay measurement was performed by using time-correlated single-photon counting method. The apparatus was assembled based on previous paper<sup>15</sup>. Laser excitation at 375 nm was achieved by a diode laser (PicoQuant, LDH-P-C-375) droved by a power control unit (PicoQuant, PDL 800-B) with a repetition rate of 2.5 MHz. Temporal profiles of fluorescence decay were recorded by using a microchannel plate photomultiplier (Hamamatsu, R3809U) equipped with a TCSPC computer board module (Becker and Hickl, SPC630). Full-width at half-maximum (FWHM) of the instrument response function was 51 ps. Criteria for the best fit were the values of  $\chi^2$  and the Durbin-Watson parameters, obtained by nonlinear regression<sup>17</sup>.

The absorption spectra of *p*-G1 in c-Hex and DMF exhibited similar spectral profile having maxima at 361 and 365 nm, respectively, as shown in Fig. 2 (a). The slightly red-shifted spectrum in DMF relative to that in c-Hex was observed. The fluorescence spectrum of *p*-G1 in c-Hex had vibrational progression with two distinct maxima at 401 and 425 nm accompanied by a shoulder at 447 nm. Those in DMF were 405, 429 and 456 nm. Although the vibrational progression of *p*-G1 in c-Hex was similar to that in DMF, the ratio between corresponding maxima was different from each other. Since this difference was found not in absorption spectra but in fluorescence spectra, the excited state seems to be more sensitive to properties of solvent than the ground state. The absorption and fluorescence spectra of *p*-G2 in c-Hex and DMF showed quite similar behavior except for a peak at 308 nm attributed to peripheral phenylacetylene moiety and slightly red-shift relative to *p*-G1. The difference between *p*-G1 and *p*-G2 may originate from delocalization of  $\pi$ -electron leading to  $\pi$ -conjugation from the phenylacetylene to a core stilbene moiety.

**Table 1.** Fluorescence lifetime of *p*-G1 and *p*-G2 in cyclohexane and DMF with excitation at 375 nm

Solvent		$\tau$ / ps					
		400 nm		455 nm		500 nm	
c-Hex	<i>p</i> -G1	9	(-0.95)	15	(-1.00)	14	(-0.98)
		723	(1.00)	730	(1.00)	804	(1.00)
	<i>p</i> -G2	8	(-0.93)	12	(-1.00)	9	(-0.91)
		635	(1.00)	648	(1.00)	732	(1.00)
DMF	<i>p</i> -G1			25	(-0.16)	16	(-0.77)
		780	(1.00)	782	(1.00)	789	(1.00)
	<i>p</i> -G2	104	(0.22)	19	(-0.32)	27	(-0.44)
		716	(0.78)	708	(1.00)	713	(1.00)

Normalized pre-exponential factors are shown in parentheses.

Table 1 lists fluorescence lifetimes obtained by the analysis of measured decay curves both in c-Hex and DMF. In the present experiment, we could not observe significant differences in rise time between *p*-G1 and *p*-G2 both in c-Hex and DMF due to the limited time resolution arising from the pulse duration of laser diode. However, at least one can postulate that fluorescence decay curves observed at all wavelengths contain distinct rise components

indicating that there is a precursor having no emission. Since the rise constant of *p*-G2 is  $\sim 30$  ps and faster than that of *p*-G1, ethynyl-BuPh may affect the relaxation time constant of Frank-Condon state of *p*-G2.

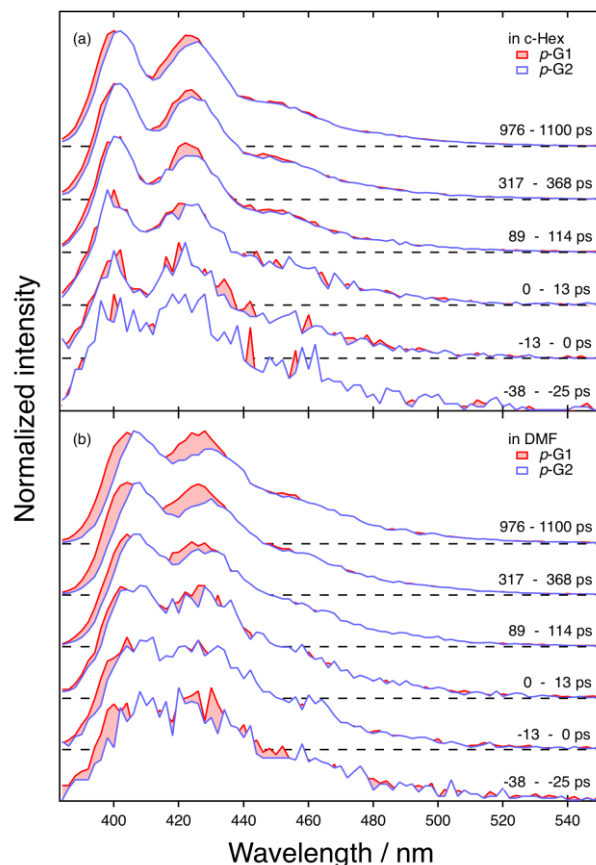


**Figure 3.** Time-resolved emission spectra of *p*-G<sub>n</sub> in DMF and cyclohexane excited at 375 nm.

Figure 3a shows the time-resolved fluorescence spectra of *p*-G1 and *p*-G2 in c-Hex with excitation at 375 nm in the wavelength range 384 to 550 nm. Obvious emission maximum and the shoulder were observed at 400, 425 and 450 nm just after excitation. The time evolution of fluorescence spectra showed slight changes in spectral shapes as well as the maximum emission wavelengths. While the peak wavelengths of *p*-G1 agreed with those of *p*-G2 just after excitation, the spectra of *p*-G2 gave gradual changes in the spectral shape in contrast to about 2 nm-shift of *p*-G1 within 1 ns. The intensity ratio between 400 nm and 425 nm also remained constant only for *p*-G1. This indicates that some sort of conformational changes takes place in the excited singlet state especially for *p*-G2 in comparison with *p*-G1. Although a rise component with 15 ps was found in *p*-G1 from lifetime analysis, the corresponding spectrum could not be identified due to the observation limit. The time-resolved spectra of *p*-G<sub>n</sub> in DMF are also shown in Figure 3b in the same measurement condition as Fig. 3a. While the time evolution of emission spectra of *p*-G<sub>n</sub> in Fig. 3b was similar to that in c-Hex with respect to red-shift of *p*-G2, the amount of red-shift of *p*-G2 relative to *p*-G1 was larger than that in c-Hex as shown in Fig. 3b. In addition, the intensity ratio of *p*-G2 between 405 nm and 430 nm significantly changed relative to *p*-G1 along with the spectral shape. This indicates that *p*-G2 can take more ionic structure than *p*-G1 due to peripheral moieties, which can interact core part in the emissive state by elongated  $\pi$ -conjugation from the peripheral phenylacetylene moiety.

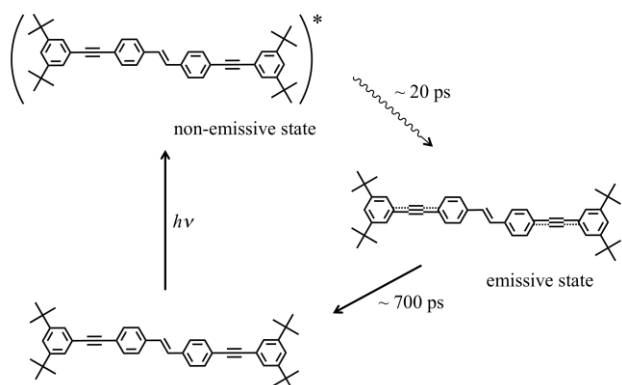


**Figure 4.** Conformational relaxation process of *p*-G1 via the excited state.

It may explain that the amount of red-shift and spectral broadening is relatively small, since *p*-G2 has no push-pull substituent because of the symmetrical structure.

Remarkable polarity-dependent fluorescence spectra suggested that the emissive states of *p*-G1 and *p*-G2 have more polar structure than the ground state. The time-resolved spectra showed that the time evolution of emission spectra of *p*-G2 was more largely red-shifted than that of *p*-G1 accompanying remarkable changes in spectral shape especially in DMF. From the above results Fig. 4 is considered for the overall scheme involved in photoexcitation. The 375nm-excitation generates non-emissive state having time constant of ~20 ps since corresponding decay time constant was not observed. The emissive state may have elongated charge-delocalized structure from the peripheral phenylacetylene moiety to a core stilbene moiety to some extent. The symmetrical structure may be responsible for limited changes in time-resolved spectra even in highly polar solvent, DMF. Whereas validity of differences in rise time constants is still unknown due to the limited time-resolution, decay time constants clearly indicate that the emissive states of *p*-G1 and *p*-G2 in DMF are more stable than in *c*-Hex. This supports that the emissive state is allowed to take an ionic structure.

Consequently, we revealed relaxation dynamic process in the excited state of *p*-G1 and *p*-G2 and solvent effect on the emissive state including corresponding time constants. This could be a basic finding for elucidating more complex dendrimer molecules.

**KEYWORDS:** phenylacetylene; dendrimer; fluorescence; time-resolved spectroscopy; relaxation kinetics

Received December 1, 2014; Accepted December 13, 2014

#### ACKNOWLEDGEMENT

We thank Mr. M. Kamada for sample preparation.

#### REFERENCES AND NOTES

1. Grimsdale, A. C.; Müllen, K. *Angew. Chem. Int. Ed.* **2005**, *44*, 5592-5629.
2. Chen, L.; Li, C.; Müllen, K. *J. Mater. Chem. C* **2014**, *2*, 1938-1956.
3. Wang, C.; Dong, H.; Hu, W.; Liu, Y.; Zhu, D. *Chem. Rev.* **2012**, *112*, 2208-2267.
4. Lupton, J. M.; Samuel, I. D. W.; Beavington, R.; Burn, P. L.; Bäslér, H. *Adv. Mater.* **2001**, *13*, 258-261.
5. Qu, J.; Pschirer, N. G.; Liu, D.; Stefan, A.; De Schryver, F. C.; Müllen, K. *Chem. Eur. J.* **2004**, *10*, 528-537.
6. Lupton, J. M.; Samuel, I. D. W.; Burn, P. L.; Mukamel, S. *J. Phys. Chem. B* **2002**, *106*, 7647-7653.
7. Ranasinghe, M. I.; Murphy, P.; Lu, Z.; Huang, S. D.; Twieg, R. J.; Goodson III, T. *Chem. Phys. Lett.* **2004**, *383*, 411-417.
8. Speiser, S. *Chem. Rev.* **1996**, *96*, 1953-1976.
9. Scholes, G. D.; Ghiggino, K. P.; Oliver, A. M.; Paddon-Ro w, M. N. *J. Phys. Chem. B* **1993**, *97*, 11871-11876.
10. Scholes, G. D.; Andrews, D. L. *J. Chem. Phys.* **1996**, *107*, 5374-5384.
11. Amatatsu, Y.; Hosokawa, M. *J. Phys. Chem. A* **2004**, *108*, 10238-10244.
12. Polialov, E. Y.; Chemyak, V.; Tretiak, S.; Mukamel, S. *J. Chem. Phys.* **1999**, *110*, 8161-8175.
13. Saltiel, J.; Kumar, V. K. R. *J. Phys. Chem. A* **2012**, *116*, 10548-10558.
14. Goodson, T. *Annu. Rev. Phys. Chem.* **2005**, *56*, 581-603.
15. Nishimura, Y.; Kamada, K.; Ikegami, M.; Nagahata, R.; Arai, T. *J. Photochem. Photobiol. A* **2006**, *178*, 150-155.
16. Lucas, N. T.; Notaras, E. G. A.; Cifuentes, M. P.; Humphrey, M. G. *Organometallics* **2003**, *22*, 284-301.
17. Boens, N.; Tamai, N.; Yamazaki, I.; Yamazaki, T. *Photochem. Photobiol.* **1990**, *52*, 911-917.